Journal of Computational Science, Volume 53, July 2021, Article number 101403
DOI:10.1016/j.jocs.2021.101403

Numerical modelling study of a modified sandbag system for ballistic protection

B Thawani[1], R Hazael[1] and R Critchley*[1,2]

[1] Centre for Defence Engineering, Cranfield University, Defence Academy of the United Kingdom, Shrivenham, SN6 8LA

[2] University of the West of England, Engineering Design and Mathematics, Frenchay Campus, Coldharbour Lane, Bristol, BS16 1QY

*Corresponding author: rich.critchley@uwe.ac.uk

ABSTRACT

Modern field fortification systems are very large and cause a logistical burden during setup, thus setting the requirement for their modification. A simulation study was conducted to study the correlation between the compaction of sand and the energy absorbed by it when impacted by a solid steel projectile at 850m/s. Furthermore, the sandbag was modified by the addition of plates in the system to observe the change in projectile penetration and the energy absorption behaviour of the sand. The factors considered for this study were the plate thickness (15mm, 25mm), plate material (aluminium, concrete, plexiglass, polycarbonate, steel) and plate location (226mm, 236mm, 256mm from the point of impact). It was observed that a layer of compressed sand is formed around the projectile, aiding the energy absorption and dissipation process during impact. Upon addition of the plate, it was observed that the modified system (plate and sand) absorbed maximum energy when the plate is placed closest to the point of maximum penetration without the plate. It was also noted that the addition of the plate enhanced energy absorption characteristics of the system compared to conventional sandbags because of increased compaction of sand. From the study, it was observed that the plexiglass and polycarbonate plates had the maximum energy absorption and maximum deformation. The steel plate had the least energy absorption and minimal deformation. Concrete and Aluminium had comparable areal density, energy absorption and lowest deformation, making them the preferred choice of plate material for a modified sandbag. The numerical studies were verified using a gas gun and a modified sandbag with Aluminium plates to show that the addition of a plate improves compaction behaviour of sand. Keywords: Compaction; Energy Absorption; Sandbag; Simulation; Ballistic plate

INTRODUCTION

The paradigm shift setting up warfare in a more urban environment has shown that the major threats that need to be protected against, are that of blast, fragment (because of blast) and ballistic attack. The shift in the use of explosives in conflicts has drastically increased the need for protection against these threats. Over the years, the two major types of protection systems that have been used for the protection of buildings are “hard and massive”, and “ductile and dynamic” systems [1]. The major requirement for any protection system is that it must be engineered to match, and defeat a given threat. This essentially implies that the design of a protection system requires the system to respond to the dynamic loads (blast and fragments) such that it is not easily defeated or too overmatched (where the whole system is displaced by the load) [1]. In terms of the engineering, a ballistic protection system needs to rapidly dissipate the energy of an incoming projectile while limiting its movement within the material.

Sand has been used as a means of protection against blast and ballistic threats for a variety of reasons which are (i) it is ubiquitous; (ii) it is cheap and can be bought in bulk quantities; (iii) it absorbs and dissipates energy effectively; (iv) it has a very high critical velocity; and (v) it is easy to work with and requires little processing before being used in the field [1,2]. The increased dependency on explosive weapon systems developed the need for larger field fortifications which raised questions for the use of sand in these protection systems.

Sand is used in fortification systems because of its increased penetration resistance when it is compacted [1,3]. The process of compaction displaces the air from the sand, resulting in reduced pore spaces between grains of sand [4]. The reduced volume due to the grain rearrangement increases the particle friction between grains resulting in the increase in shear strength of the sand [4]. The increased shear strength results in the increased penetration resistance of sand [3,4]. Additionally, the increased particle friction has a direct influence on the ability of the sand to absorb and dissipate the energy from the incoming projectile. While sand can resist projectile penetration due to particle friction, it uses the process of compaction to resist the attack from blast. The major threat from blast

is the propagation of the shockwave through the material [4,5]. Sand resists blast by undergoing densification due to the pressure load from the shockwave [6,7]. The process of compaction increases the contact between particles, allowing the dissipation of energy from the propagating shockwave [7–9]. More recently, sand has found application as a common infill in protective systems such as HESCO. The HESCO system typically holds the sand (up to 14.77 metric tonnes) in a high specification mesh and geotextile framework [10]. These systems are very robust and have the capability to defend against a large array of direct and indirect threats such as fragments, bullets and shockwaves from blast [4]. Furthermore, the barriers still face the risk of being displaced when subjected to blast which in turn increases the risk of collateral damage to personnel [11]. In addition to this, there have been multiple studies done to show that geoparticles larger than sand are more effective at responding to a ballistic threat [12–14]. Moreover, these kinds of barriers are mainly suited for military applications primarily due to their size and the space required for their setup.

With such a dependence upon systems such as HESCOs, extensive study involving projectile impact into sand have been conducted experimentally [4,11,13,15–17]. The primary aim of these studies is to observe the penetration resistance provided by sand and how the physical properties of sand play a role in protecting against ballistic attack [15–17].

While experimental impact studies allow for a clear observation of the response of sand to dynamic loading, they pose a challenge with regards to the quantification of this response [6]. The use of sensors and high speed cameras along with processes such as digital image correlation have been used in recent years to measure the response of sand to impact and study its energy absorption characteristics [8]. The caveat with this experimental method is the cost of equipment and the increased source of human error given the increased complexity of the setup [6,18]. Furthermore, the challenge with an experimental method is the pre-processing (drying and mixing of sand to ensure a uniform measure of moisture throughout the sample) of material required to ensure a uniform setup, coupled with the opaque nature of sand. Additionally, studies often

use gas guns to fire projectiles with simplified geometries as opposed to real ballistic firings, resulting in a further simplified response.

While experimental methods hold their value, numerical methods are a cost-effective approach to recreate similar scenarios and observe material behaviour. With the case of sand, the use of numerical methods enables the user to observe the compaction behaviour of sand and energy transfer mechanism when it is impacted by the projectile [6,11,19]. The primary advantage of using numerical methods for studying impact is that it is not resource heavy. It also allows the direct visualisation of the behaviour of the impacted sand and to accurately quantify the response of sand under loading [7,20,21]. Furthermore, the use of numerical methods increases the versatility of the study because it allows the user to easily work with a variety of materials and geometries for the same impact problem. Finally, it is safer as high-energy events are simulated rather than physically produced. The use of numerical modelling allows for more research to be conducted as opposed to physical testing where specialist facilities are required. In any case, the use of numerical methods, still requires some experimental studies to validate the results generated. This is because material models can have inaccuracies or incomplete data which can result in a discrepancy between simulation and experimental results.

The change in threat profile creates a logistic and financial burden with regards to the use of current protection systems due to their large size and filling requirement. A simple method to navigate around this issue is to increase the areal density of the protection system. Adding a plate to a sandbag will change its areal density because a portion of the sand is replaced by a solid plate. The areal density of the protection system is an important factor used to measure the effectiveness of a protection system. Adding a plate can reduce the size (while maintaining the areal density) of the system or increase its areal density (while maintaining its size). The objective of this study is to observe the change in energy absorption characteristics of the protection system after the addition of plates to an existing sandbag design. The variables being considered are (i) position of plate inside the sandbag; (ii) plate thickness; and (iii) plate material.

The position of the plate influences the compaction of the sand and the confinement of the plate increases its resistance to ballistic attack. The plate material influences the failure mechanism and the energy absorption characteristics of the system. This study focuses on the compaction behaviour of sand and how it changes with the presence of a large object in the system. Previously, studies have focused on the physical properties of sand and how they influence the penetration resistance of the system [2,4,6,13,17,22]. Observing the compaction behaviour and how it changes by modifying the sandbag creates the opportunity to improve the protection system performance with minimal changes to the filling.

1 METHODS AND MATERIALS

1.1 Choice of Materials

For simulation studies, materials are assigned their properties using Equations of State (EOS), strength models and failure models. The EOS defines the thermodynamic response of the material to loading. The strength model defines the mechanical response of the material to loading and the failure model defines the limits after which the material fails. Table 1 shows the materials used for the simulation, their EOS, strength models and their failure models. Sand is ubiquitously used in hard and massive protection systems thus making it the obvious choice for filler material for this model. Subsequently, steel 1006 is the preferred material for the projectile based on previous work done on protection against impact [11]. Aluminium has been chosen as a target plate material due to its prior use in armour systems for vehicles [23]. Furthermore, concrete has been considered as plate material because of its good energy absorption characteristics and its prior use in ductile and dynamic protection systems [1,24]. Plexiglass and polycarbonate have historically been used for personal protection systems, making them viable candidates for a target plate in this system. Finally, steel 4340 was chosen as a plate material because it has also been previously used in structural protection systems [11].

Table 1 Summary of material models and properties

Material	Sand	Steel 1006	Al 6061-T6	Concrete (35Mpa)	Plexiglass	Polycarbonate	Steel 4340
EOS	Compaction	Shock-Linear	Shock-Linear	P-Alpha	Shock- Linear	Shock- Linear	Linear
Density (g/cm^3)	1.674	7.896	2.70	2.75	1.186	1.2	7.83
Yield Stress (kPa)	$2.26x10^5$	$3.5x10^5$	$2.9 x 10^5$	$3.527x 10^4$	$6.5x10^4$	$8.06x10^4$	$4.7x10^5$
Strength model	MO Granular	Johnson-Cook	Steinberg-Guinan	RHT Concrete	-	Piecewise JC	Johnson-Cook
Failure model	Hydro P_{min}	-	-	RHT Concrete	-	Plastic Strain	Johnson-Cook
Reference	[25]	[26]	[27]	[28,29]	[30]	[31]	[32]

1.2 Model Setup

ANSYS AUTODYN 2020 R1 was used to simulate the models for this study. Figure 1 shows the AUTODYN-2D model setup used to simulate a projectile impacting into sand. To reduce computational resources the model represents only a localised section (300mm x 300mm) of the whole sandbag. Free flow conditions were assumed for sand particles that exit the edges of the model. The steel 1006 projectile has a 12mm diameter and a velocity of 850m/s. Projectile velocity of 850m/s is equivalent to the velocity of a 12mm spherical fragment from a 155mm artillery shell at 11.7m (based on Gurney equations – Appendix A). The thickness of the plates (15 and 25mm) was selected based on previous work with composite armour systems [12,33,34]. The location of the plate was decided based on the maximum penetration of the projectile in the sand and the size of the compacted section of sand ahead of that point. In this study, the plate is placed at three different points (226mm, 236mm and 256mm) in the compacted sand along the horizontal axis in line with the point of impact (Figure 2). These specific locations for the plate have been selected because the plate is not

subject to impact given the timescale of the simulation. Furthermore, it helps elucidate the response of the plate to compressive loading and the change in its specific internal energy with respect to time. Placing the plate in the region of compressed sand aids in observing the change in behaviour of compressed sand when interacting with a solid body.

According to the fidelity study (discussed later in this section), compaction of sand was observed up to 40mm ahead of the maximum penetration depth. Based on that finding, the plate was placed 10, 20 and 40mm ahead of the maximum penetration depth to observe the change in compaction behaviour.

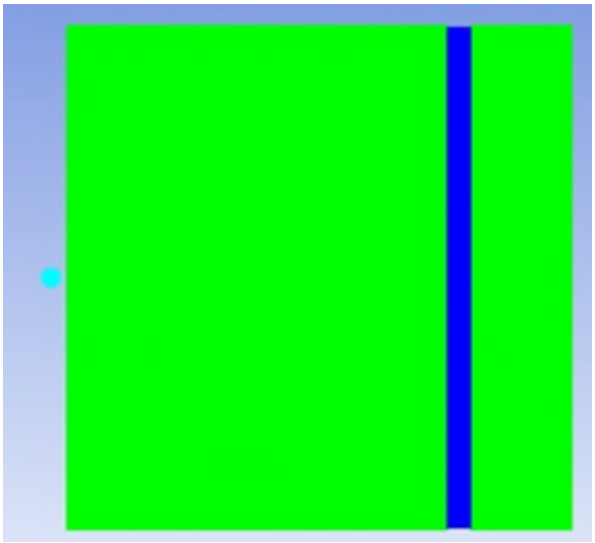

Figure 1 AUTODYN 2D model setup (Legend: Sand – Green; Plate – Blue; Projectile – Cyan)

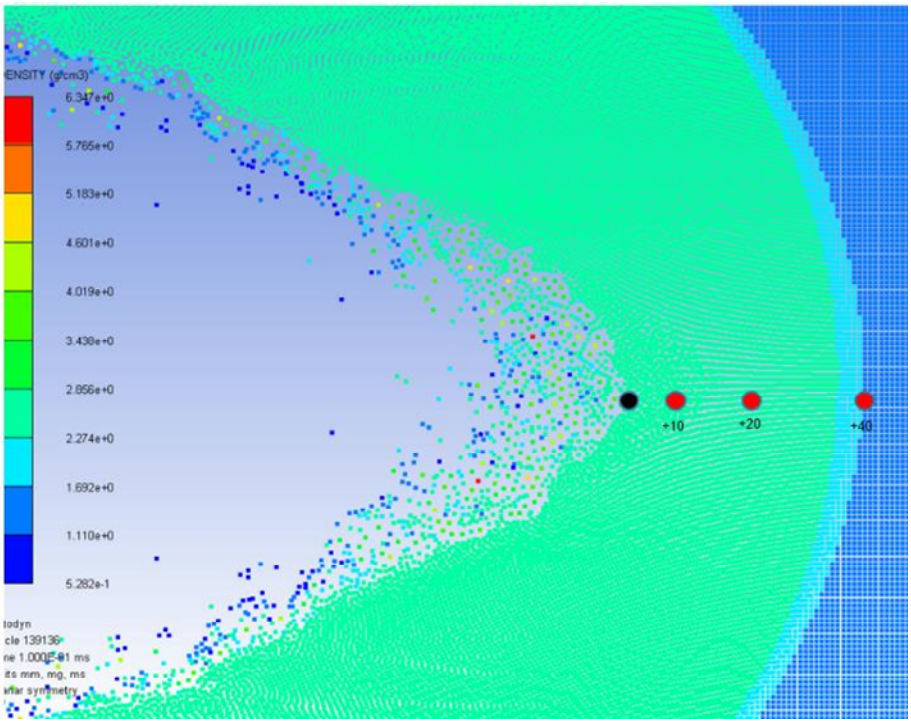

Figure 2 Plate locations within compressed sand: Black dot - Point of maximum penetration (216mm); Red dots - plate locations (226, 236 and 256mm)

1.3 Solver Selection

The Eulerian solver is characterized by a fixed observation domain though which bodies/particles move [35]. A finite difference method is used to observe the flow of mass, momentum, and energy in the continuum. This is possible because the mesh does not move, and difference equations can be used to calculate the change in properties and material location between nodes [35]. In the Lagrangian solver, the observation domain is fixed relative to a moving body/particle. This implies that, contrary to a Eulerian mesh, the mesh in a Lagrange solver is attached to the model [35]. In this model the mass, momentum, and energy are transported through the material cells as the materials move through the continuum. A finite element method is used to compute the flow of mass, momentum, and energy within the system [35,36]. Smoothed Particle Hydrodynamics (SPH) was originally invented for the simulation of astrophysical phenomena to observe the arbitrary movement (in 3 dimensions) of particles

without limiting boundaries. The flow of mass, momentum, and energy is measured at the particle positions by calculating a weighted average of the values of the local particles [37]. As a result of this, the discrete particles are “smoothed” over while maintaining a fixed mass in a finite volume [35,38].

Based on the different kinds of solvers, the model setup requires the use of one or more kinds of code to adequately compute and generate reliable results. The same solver cannot accurately represent all types of material due to the different EOS, strength and failure models assigned to them. The primary considerations while selecting a solver for an impact problem are (i) expected deformation of material(s); (ii) freedom of movement of particles of a given material; and (iii) computational requirement of the model (i.e. how computationally heavy the model is). Based on this criteria, three solvers were considered for the computation of this problem (i) Euler; (ii) SPH-Euler; and (iii) SPH-Lagrange. Figure 3 shows sample results of the same model being computed with different solvers.

Figure 3a shows the computation of the model with a Euler solver. As mentioned earlier, the Euler solver allows for large deformations in impact problems while not being too computationally heavy. The caveat with that is the scope for inaccuracy when simulating the failure of solid materials like metals. Subsequently, this solver functions under a constant density condition in a fixed mesh. This implies that the particles within this mesh move freely while ensuring that the material density remains constant. From Figure 3a, the density of the sand does not change upon impact, except a minute amount of densification at the interface where the projectile interacts with the sand. Observations from experimental studies show that sand undergoes densification upon impact. Therefore, the use of a Eulerian solver for the computation for this problem is not adequate.

Figure 3b shows the computation of the model with a SPH-Euler solver. In this model, the sand is modelled with a SPH solver and the plate is modelled with a Euler solver. Modelling the sand in the SPH solver enables the sand to move with a larger degree of freedom while allowing the particles of sand to interact with

each other. Due to the computational model of the solver, it is possible to observe the densification and compaction behaviour of sand during an impact loading event. This model is not computationally heavy, but the SPH and Euler solvers are not compatible because the SPH is essentially mesh-free whereas the Euler solver has a rigid mesh. The Euler solver has a constant mass and all the interaction is limited to the boundaries set by the mesh. As a result, it cannot compute material interactions with particles in a SPH mesh. As a result, the SPH-Euler solver cannot be used to compute the model.

Figure 3c shows how a SPH-Lagrange solver computes the model. Like the SPH-Euler solver, the sand is modelled with a SPH solver whereas the plate is modelled with a Lagrange solver. This solver computes the impact problem with the most accuracy amongst the three solvers being compared. The challenge accompanied with the accuracy is that the solver is computationally heavy, resulting in a large time consumption for each simulation. Unlike the SPH-Euler solver, the SPH-Lagrange solver does not face a compatibility problem because both, SPH and Lagrange, solvers are based on a finite element method for computing the flow of mass, momentum and energy [36,38].

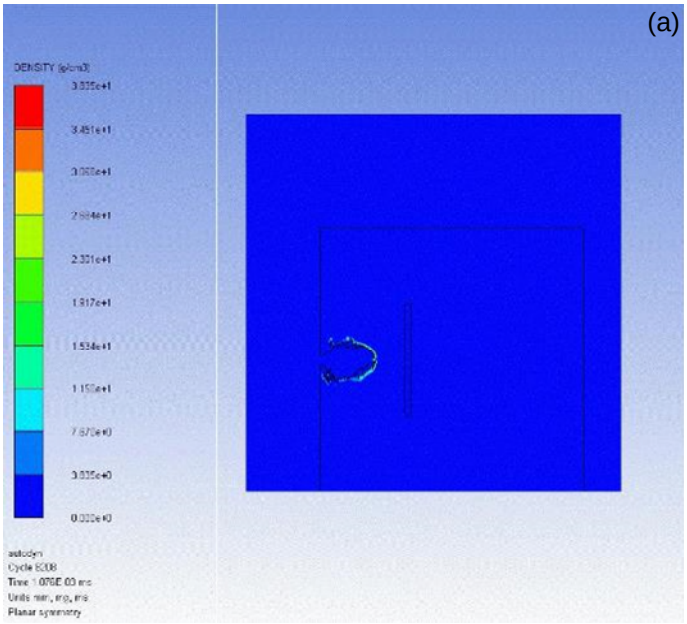
(a)
DENSITY (g/cm3)
autodyn
Cycle 6208
Planar symmetry

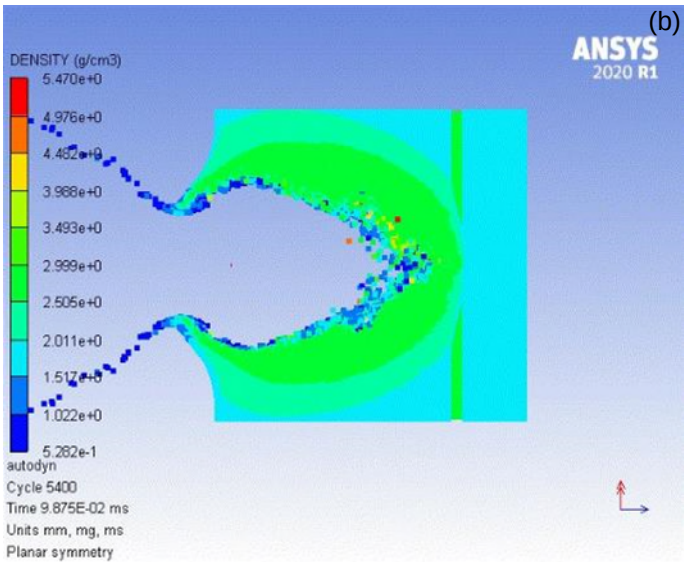
(b)
ANSYS
2020 R1
DENSITY (g/cm3)
5.470e+0
4.976e+0
4.482e+0
3.988e+0
3.493e+0
2.999e+0
2.505e+0
2.011e+0
1.517e+0
1.022e+0
5.282e-1
autodyn
Cycle 5400
Time 9.875E-02 ms
Units mm, mg, ms
Planar symmetry

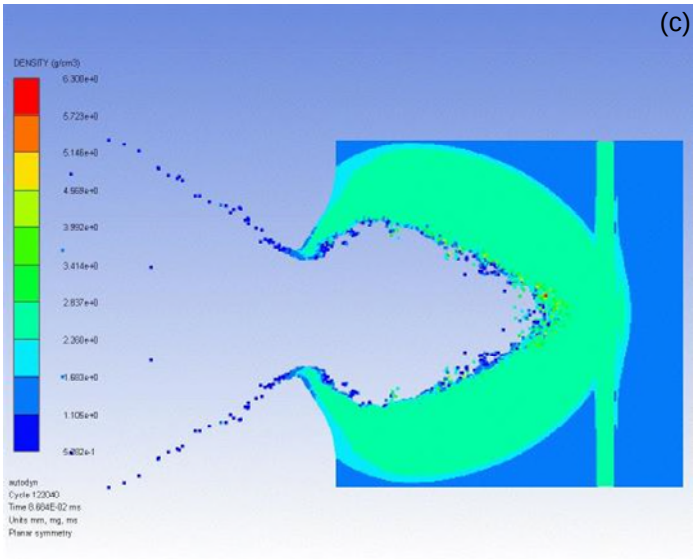

Figure 3 Solver selection for 12mm steel projectile impacting sandbag at 850m/s with 15mm/25mm plate at 226mm/236mm/256mm: (a) Euler solver; (b) SPH - Euler Solver; (c) SPH - Lagrange Solver

1.4 Fidelity Study

To optimise computation time without compromising accuracy, a fidelity study was undertaken. Since the SPH-Lagrange solver has been selected, it must be noted that the particle size (smoothing length) of the SPH elements defines the mass and density of the filling. This in turn, directly influences the computational time of the problem. For this type of model, the particle size influences the penetration depth of the projectile in sand. Table 2 shows the observations from the fidelity study.

Table 2. Summary of Fidelity Study

Smoothing length (mm)	Computation time (h)	Completion	Penetration depth (mm)
0.5	72+	8%	142*
1	9	100%	216
2	1.5	100%	456

***** Represents the penetration depth at the time of model stop.

From the fidelity study, it can be demonstrated that a smoothing length of 1mm is the ideal choice for the modelling of sand in the model. The model with

smoothing length of 0.5mm was expected to take approximately 900 hours to converge using extrapolation methods. While this model provides the highest fidelity, it is too computationally intensive and not very feasible. When smoothing length 2mm is used, the fill density reduces drastically resulting in the sand being completely overmatched by the threat. Additionally, the 1mm smoothing length ensures adequate fill density to represent the compaction of sand during the filling process. 1mm smoothing length enables an accurate representation of existing sand-based protection systems.

1.5 Validation of Simulation Results

The simulations were experimentally verified in a lab setup. A 30mm bore light gas gun was used to fire a steel projectile into sand. 56 bar helium was the driving gas used in the gun to achieve an impact velocity of 867m/s. Building sand was used in the target because of its uniform particle size and high availability. Figure 4 shows the setup of the experiment. 15mm thick Aluminium plates were selected for the validation of the simulations to ensure a uniform standard between firings and easy replication of the experiment. The sand was lightly compacted into the box to replicate the setup of modern HESCO sandbags. 2 shots were fired in the presence of a plate and 2 shots were fired without the presence of a plate to validate the observations from the simulations.

Figure 4 Experiment setup for gas gun firings into sandbag target with Aluminium plate at 226mm from point of impact

2 RESULTS AND DISCUSSION

2.1 Compaction Behaviour of Sand

Sand is subjected to dynamic loading (compressive and mechanical loading) when it is impacted with a projectile travelling at 850m/s [14]. Due to the granular structure of sand, it tends compact and densify when it is under a compressive load [1,6,39]. Previous studies have shown a change in the energy absorption behaviour of sand as its density changes, thus implying a shift in its penetration resistance [3,7]. The plate was placed in the sandbag so that it was not impacted by the projectile given the timescale of the simulation. The selection of plate location within the sandbag and its effect on the compaction of sand is discussed in the subsequent section. The energy absorption behaviour is observed by measuring the change in specific internal energy of the material. The change in specific internal energy of the material provides an insight into the energy absorbed by it during and after the impact. Measuring the densification of the material can aid the process of developing a correlation between compaction and energy absorption. Figures 5 and 6 show the change in density of sand when it is impacted by the projectile with plates at 226mm from the point of impact. The

change in density of sand with plates at 236mm and 256mm from the point of impact is shown in the supplementary information (SI Figures 1 and 2).

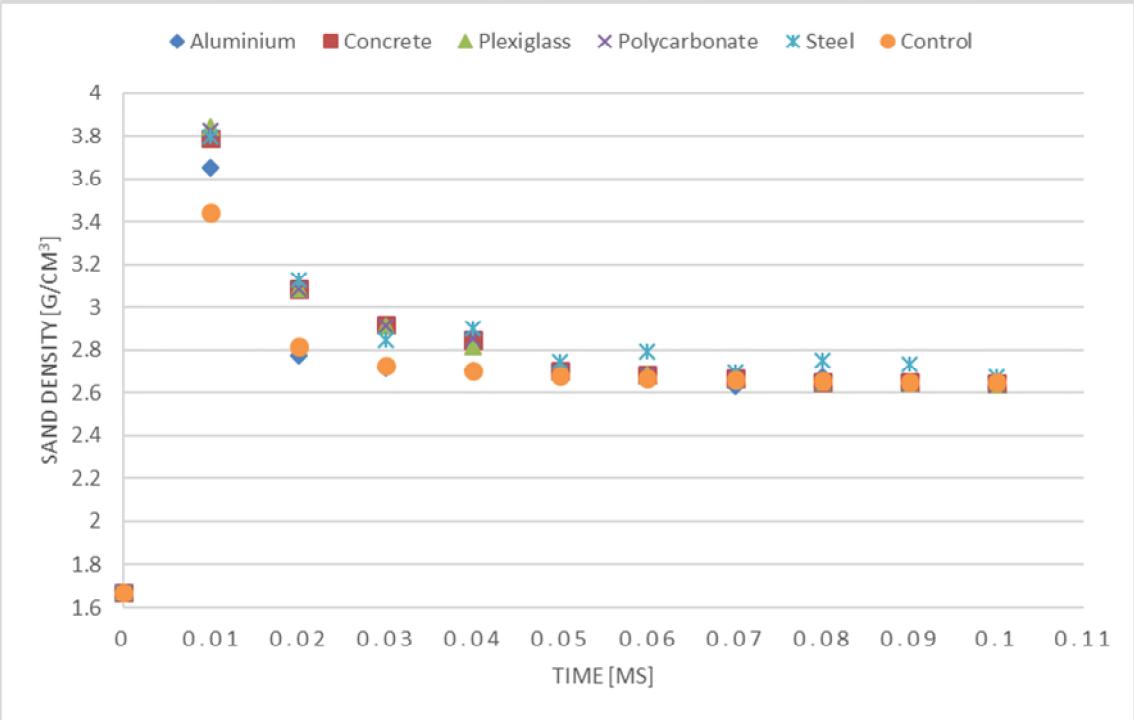

Figure 5 Change in density of sand with respect to time when impacted with a steel projectile (12mm diameter) in the presence of 15mm plate placed at 226mm from the point of impact.

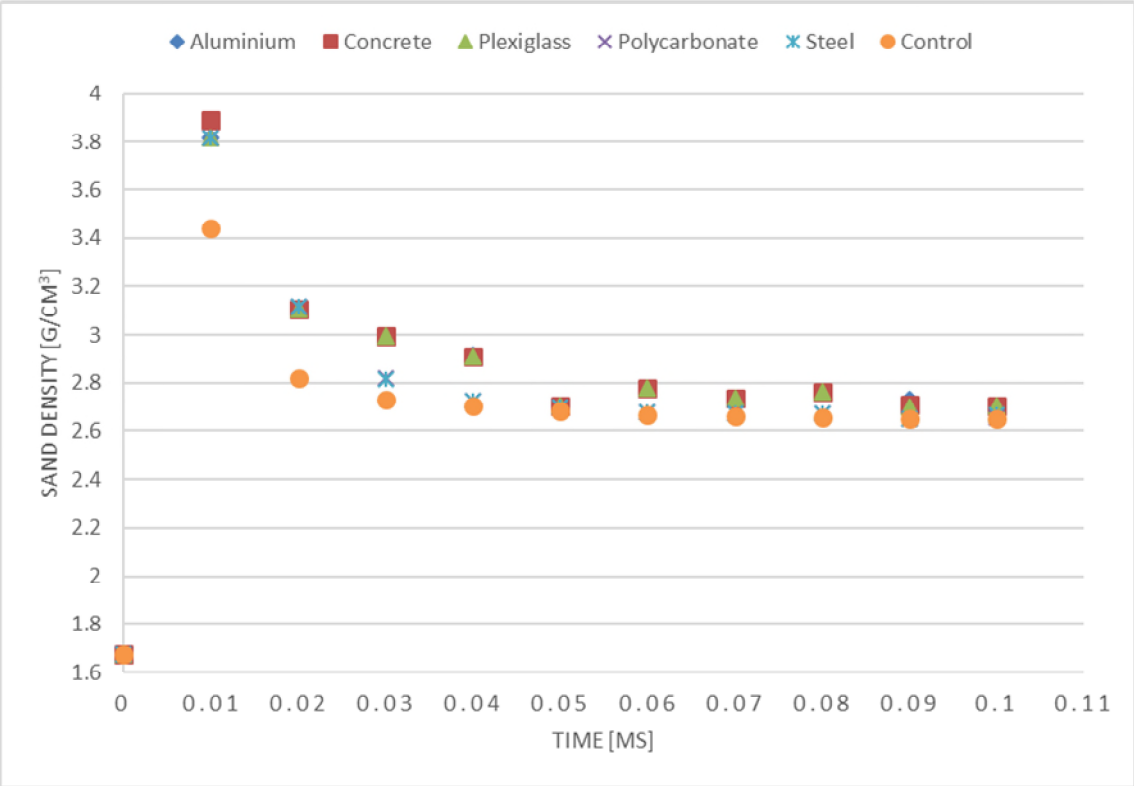

Figure 6 Change in density of sand with respect to time when impacted with a steel projectile (12mm diameter) in the presence of 25mm plate placed at 226mm from the point of impact.

All simulations showed densification of sand when impacted by a steel projectile. After the initial impact (0.01ms) in the conventional sandbag, the density of the sand increased to 3.44 g/cm^3, showing a 105% increase in sand density (Control data in Figures 5 and 6). The densification of sand around the point of impact increases as the projectile penetrates the sand until the size of the compressed area becomes constant (40mm). During this process, the density increases during impact and then reduces as the size of the compressed sand layer becomes constant. This compressed layer of sand plays a major role in the energy absorption process of the system. Sandbags with 15 and 25mm plates added to them showed an increase in sand density of up to 129% (Figure 5) and 132% (Figure 6) respectively. After initial impact (0.01ms), the sand decompresses as the energy is dissipated from the system. Here, decompression refers to the sand particles exiting the layer of compressed sand around the projectile. It must be noted that the density of the sand after decompression is

1.5% higher in the modified sandbags as compared to the conventional sandbags. It can be postulated from the data presented that the presence of a solid plate in the bag increases the densification of sand, thus influencing its energy absorption characteristics. This is because the plate creates an obstruction for the sand, causing it to compress when the plate is impacted. This compression increases the specific internal energy of sand, thus increasing its energy absorption. The energy absorption is an important factor that influences the penetration process and the penetration resistance provided by the sand [3,4]. This claim is further supported by the observation that the modified sandbags allowed a maximum penetration of 201mm as compared to the 216mm penetration in the conventional sandbags with a given timescale of 0.1ms. Since the timescale is too small, the penetration in the modified sandbags is the same, but the energy absorbed by the sand and plate is different (discussed in Sections 3.2, 3.3 and 3.4). Furthermore, it can be noted that adding a plate to the sandbag enhances the energy absorption behaviour of the system as shown by the 22% increase in values of specific internal energy of sand as compared to a conventional sandbag. Figures 7 and 8 show the change in specific internal energy of sand before the compressed layer of sand interacts with the plate at 226mm (0.01-0.07ms). The change in specific internal energy of sand before the compressed layer of sand interacts with plates at 236 and 256mm are shown in the supplementary information (SI Figures 3 and 4).

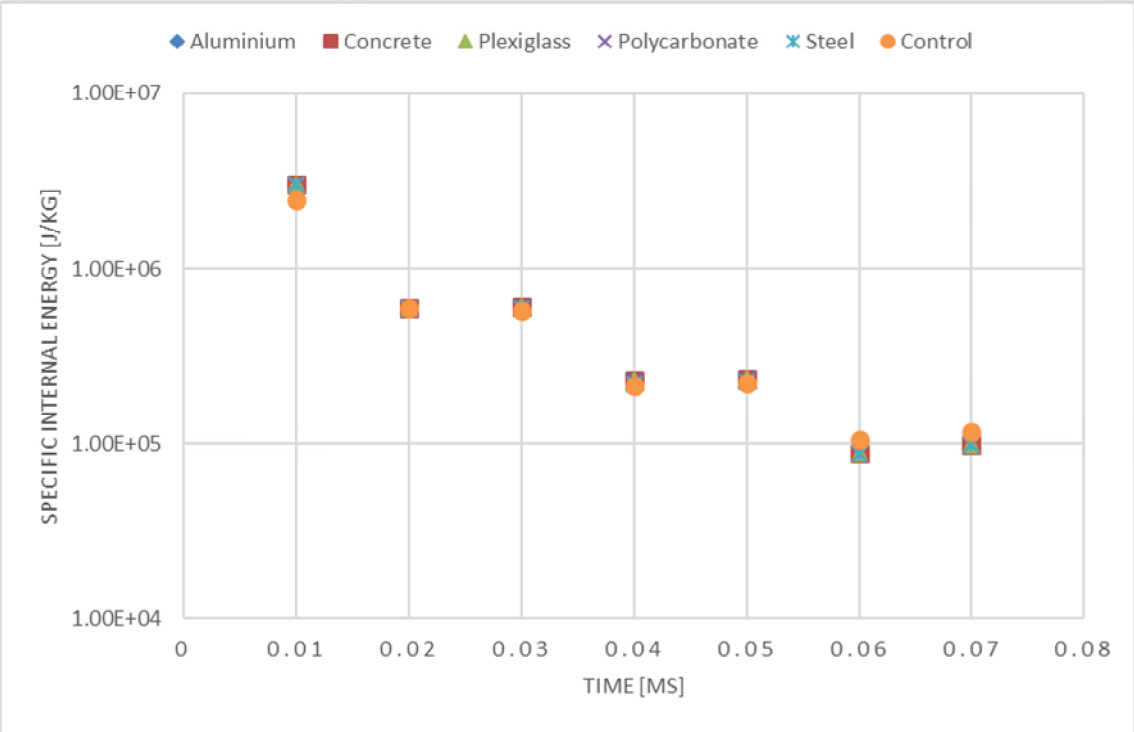

Figure 7 Change in specific internal energy of sand when impacted by a steel projectile (12mm diameter) at 850m/s in the presence of a 15mm plate at 226mm from the point of impact. 0.01-0.07ms is the time interval before the compressed sand interacts with the plate.

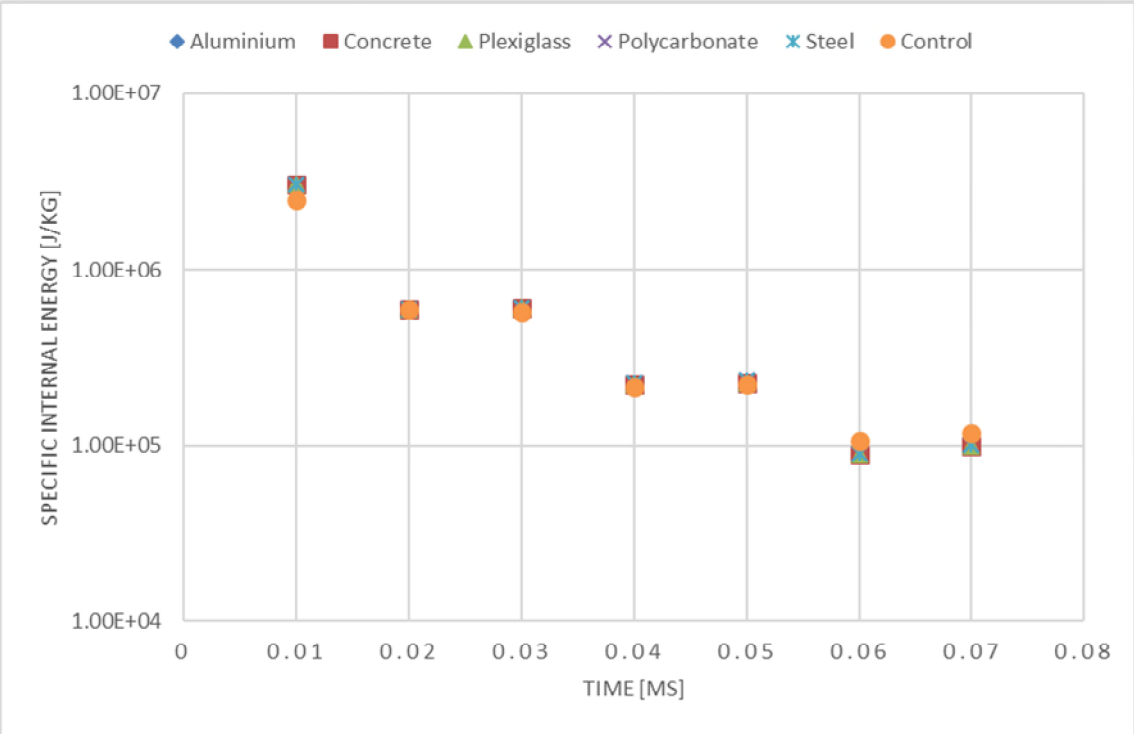

Figure 8 Change in specific internal energy of sand when impacted by a steel projectile (12mm diameter) at 850m/s in the presence of a 25mm plate at 226mm from point of impact. 0.01-0.07ms is the time interval before the compressed sand interacts with the plate.

From figures 7 and 8, it can be inferred that the addition of a plate to the sandbag increases the specific internal energy of the sand during the initial impact (0.01ms) by approximately 22%. The increased energy absorption was observed in all modified systems irrespective of the plate material, location, or thickness. This is because the plate does not absorb any energy during initial impact, but the presence of the plate compacts the sand in the system. This can be linked to the increased density of the sand at 0.01ms, thus suggesting a correlation between the densification of sand and its specific internal energy. The reduction in specific internal energy of sand after the initial impact (0.02-0.07ms) can be correlated to its decompression and the subsequent dissipation of energy. The decompression of sand was observed behind the projectile as sand particles moved into the cavity created due to the impact (Figure 9). The decompression of sand particles happens because they enter a low pressure area behind the projectile. Subsequently, the shear forces on sand particle due to impact reduce

once the particle is behind the projectile, resulting in its decompression. Additionally, the initial peak in specific internal energy and its subsequent reduction can be attributed to the penetration process reaching temporary equilibrium until the layer of compressed sand is interacting with the rigid plate [39,40]. The term ‘temporary equilibrium’ refers to the equilibrium being established between the transfer of energy from the projectile to the sand and the dissipation of energy from the sand [3,4,18,39,40]. Key markers for the process reaching equilibrium were the constant size of the layer of compressed sand, and the reduced fluctuation in density as well as specific internal energy.

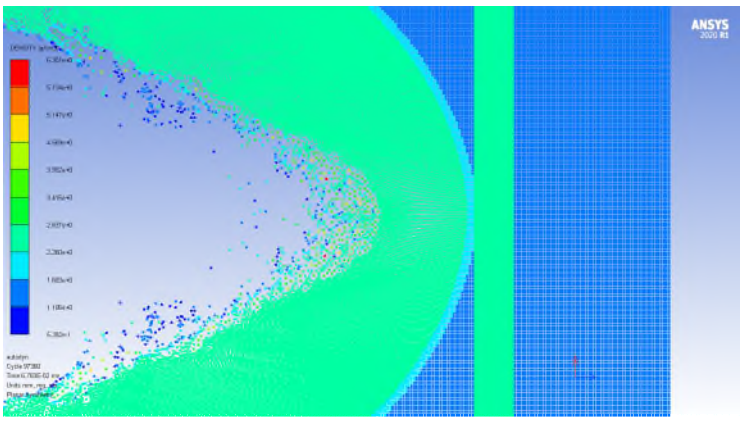

Figure 9 Decompression of sand particles observed behind the point of penetration following the steel projectile (12mm diameter) impacting sand at 850m/s with 15mm plate at 226mm from point of impact.

2.2 Effect of Distance

It was noted that the presence of a plate in the sandbag improved the system’s energy absorption performance and that the location of the plate within the sandbag plays an important role in the amount of energy absorbed by the two components of the protection system. From the simulation studies, it was observed that the front surface of the compressed layer of sand interacted with the face of the plate at 226mm, 236mm and 256mm at 0.07ms, 0.08ms and 0.1ms, respectively. In the absence of a plate in the system, the compressed sand does not interact with any obstruction resulting in lesser energy transfer out of the system. In addition to the visual observation, evidence of the interaction between the plate and compressed sand can be seen in the increase in specific

internal energy of the two interacting materials at 226 mm (Figures 10 and 11). The change in internal energy of sand (0.08 – 0.1ms) for plates at 236mm and 256mm is shown in supplementary information (SI Figures 5 and 6).

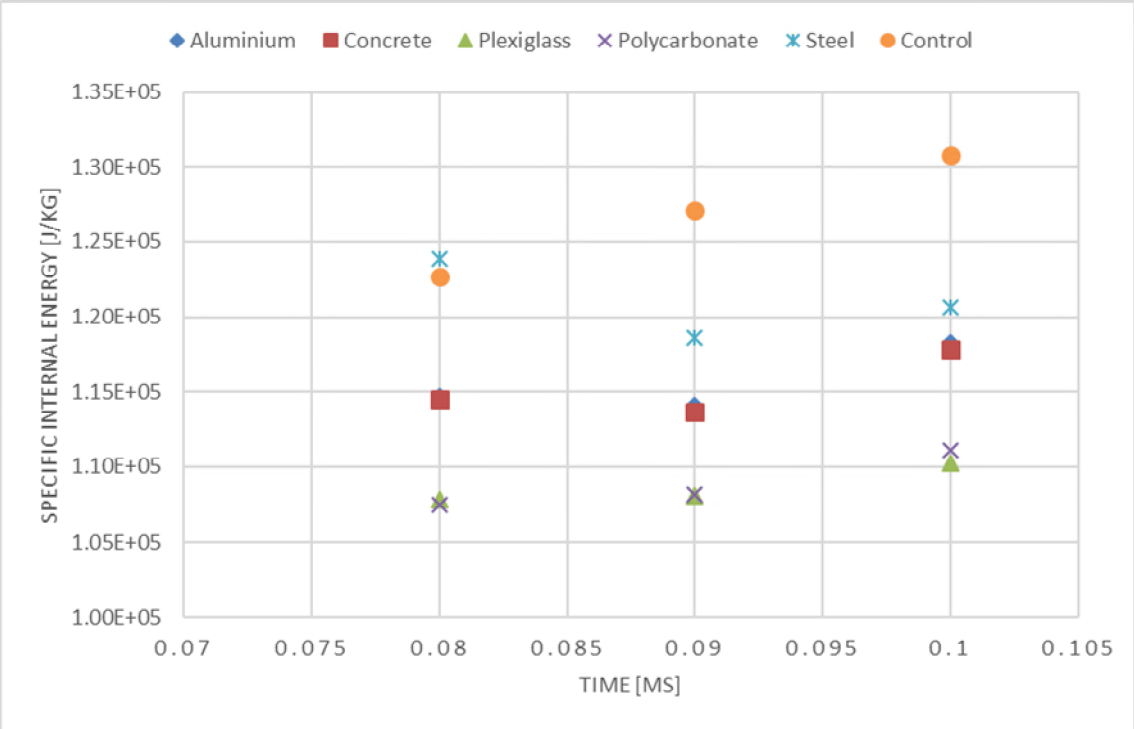

Figure 10 Change in specific internal energy of sand when impacted by a steel projectile (12mm diameter) at 850m/s in the presence of a 15mm plate at 226mm from point of impact. 0.08-0.1ms is the time interval during which the compressed sand interacts with the plate.

sand and plate. Plexiglass and polycarbonate are materials with high ductility and relatively low strength characteristics [41,42]. Due to this, these materials tend to absorb more energy while undergoing deformation. Contrary to this, materials like aluminium, steel and concrete have relatively lower ductility and can resist deformation due their high yield strength [43–45]. After the initial response of the plate and decompression of sand (after 0.08ms), the specific internal energy of sand continued to increase as the plate underwent deformation. The contact and compressive forces between the sand and plate allowed for energy dissipation from the sand to the plate. This resulted in the increase in specific internal energy of the plate material, thus suggesting the ability of the plate to aid the process of energy absorption from the penetrating projectile.

Simulations with plate locations at 236 and 256mm showed a change in energy absorption of sand at 0.08 and 0.1ms, respectively. In these cases, the energy absorbed by the sand was approximately 9% higher than the previous case because the compressed sand interacts with the plate at a later stage in the penetration process. Simulations with plate location at 236mm showed that the sand had a higher specific internal energy when it interacted with the plate and an increase in energy absorption of 1.7% after initial contact. Due to the timescale of the simulations, no observation of the decompression behaviour of sand could be made. Subsequently, simulations with the plate located at 256mm showed 3.4% increase in the energy absorption of compressed sand as it impacted the plate. The interaction of the plate and compressed sand was initiated at the wrap up time of the simulation, which creates an inaccuracy in the observation of the energy absorbed by the sand. This however allows for the observation of the energy change in different plate materials at the point of impact.

2.3 Effect of Plate Material

In addition to the location of the plate in the sandbag, the plate material plays a significant role in the penetration resistance provided by the protection system. The plate needs to be able to withstand the pressure loading from the sand while still being able to absorb the energy from the projectile. The energy absorption characteristics of the material are dependent on its molecular structure as well as

the tensile strength of the material [46]. The different materials considered for this study have different yield strengths, tensile strengths and have very different molecular structures. The yield stress of the material defines the extent to which it will elastically deform when subjected to a load [47]. This suggests that the energy absorption behaviour of these materials will be largely different from each other. Figures 12 and 13 show the change in specific internal energy of plates of different materials and thickness at 226mm from the point of impact when the layer of compressed sand interacts with the front face of the plate. The change in specific internal energy of the plate at 236mm and 256mm from the point of impact when the layer of compressed sand interacts with the front face of the plate is shown in the supplementary information (SI Figure 7 and 8).

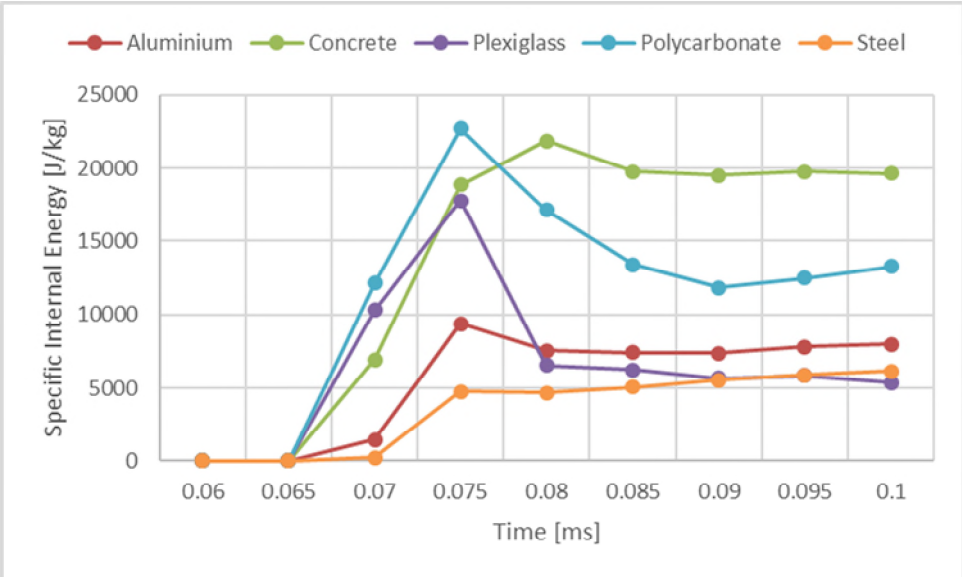

Figure 12 Change in Specific Internal Energy of 15mm plate when subjected to local load by compressed sand induced from the ballistic impact of the steel projectile (12mm diameter) at 226mmfrom the point of impact.

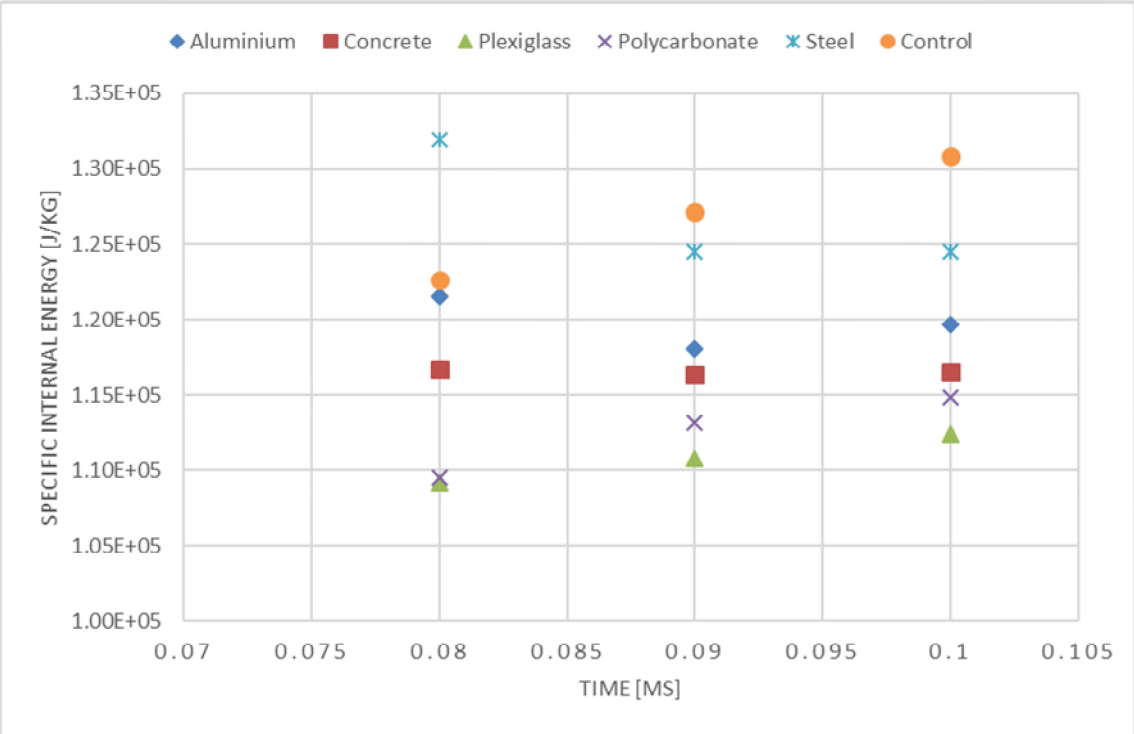

Figure 11 Change in specific internal energy of sand when impacted by a steel projectile (12mm diameter) at 850m/s in the presence of a 25mm plate at 226mm from point of impact. 0.08-0.1ms is the time interval during which the compressed sand interacts with the plate.

From Figures 10 and 11, when the compressed sand interacts with the plate, there is an increase in the specific internal energy of the sand. The change in specific internal energy of the sand at the time of impact can be attributed to the densification it undergoes due to its inertial movement, resulting in the compression of sand against the plate. This initial increase in specific internal energy was observed in all cases but at different times. For cases where the plate was at 236mm, it was observed that there was a change in the energy absorption behaviour of sand after the initial increase in specific internal energy at 0.08ms. When concrete, aluminium and steel plates were used in the system, there was a reduction in the specific internal energy of sand. The reason for this can be attributed to the temporary decompression of sand caused by the response of the plate and its backing sand. Compared to these three materials, the use of polycarbonate and plexiglass plates in the sandbag saw an increase in the specific internal energy of the sand after the initial contact of the compressed

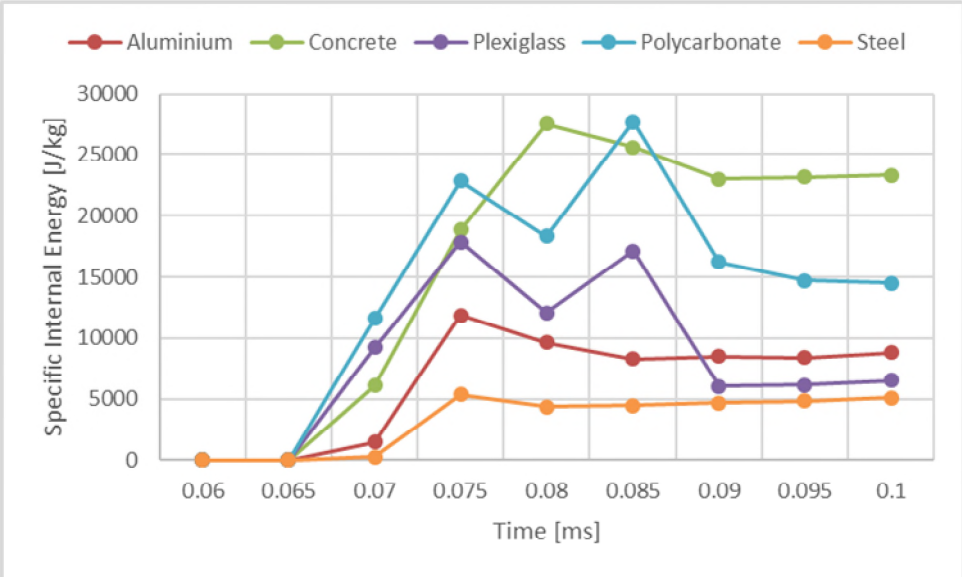

Figure 13 Change in Specific Internal Energy of 25mm plate when subjected to local load by compressed sand induced from the ballistic impact of the steel projectile (12mm diameter) at 226mm from the point of impact.

From Figures 12 and 13, the polycarbonate and plexiglass plates have 22,805 J/kg and 17,869 J/kg increase in specific internal energy - the highest energy absorption at the time of impact. The concrete and aluminium plates have the third and fourth highest energy absorption, respectively. The steel plate has the least energy absorption of all the materials being tested. Between the two metal plates, aluminium had a better energy absorption performance. This can be attributed to its relatively lower strength characteristics to steel [47]. Aluminium has a lower yield and tensile strength, resulting in the larger deformation compared to the steel plate [46,47]. The larger deformation occurs because of the material's response to the energy supplied during loading. The compressive load results in a deviatoric response, causing the plate to change shape. Steel on the other hand, has high strength characteristics and is a rigid material [11,40]. Due to this, it does not absorb as much energy and thus does not deform as much as the other plates. It was visually observed that the steel plate deformed the least and consequently had the least increase in specific internal energy. While aluminium and steel both have face centred crystal structures, steel is much denser, resulting in its relatively larger rigidity as compared to aluminium [46]. Subsequently, concrete is a very hard and stiff material due to its high yield

strength and very low tensile strength [1,39,40]. But its molecular structure is very different from the two metals, resulting in its higher specific internal energy. Concrete has a hybrid structure combining crystal layers of silica tetrahedra and amorphous layers of calcium oxide [48]. The crystal structure allows for rigidity while the amorphous component improves the energy absorption characteristics of the material. Subsequently, polycarbonate and plexiglass are both amorphous thermoplastic polymers [41,42]. Due to their amorphous nature, the materials absorb energy (through deformation) better and respond to deviatoric stress without undergoing tensile failure [41,42]. While plexiglass and polycarbonate absorb energy during an impact, their amorphous nature of the molecules results in the rapid dissipation of energy as well. This can be observed when the specific internal energy of both these materials rapidly reduces after the initial contact with compressed sand. On the other hand, concrete has a smaller reduction in specific internal energy after the initial contact with the sand, thus suggesting a higher energy absorption capacity coupled with high strength characteristics.

In addition to the plate material, the different locations of the plate resulted in different amounts of sand behind the plate. The sand behind the plate acts like a backing support and potentially influences the energy absorption characteristics of the plate and its response to the compressive loading [11]. Cases where the plate was placed at 226mm had the largest amount of backing sand. It was observed that the deformation of the plate caused a compression in the sand particles behind it. It was observed that the plate deformed due to the energy absorbed, the compressive forces are applied to the sand behind it (Figure 14). The compression of sand was observed all over the back face of the plate, but it was maximum around the region of deformation. This results in the dissipation of energy from the plate into the sand. Because of sand's high energy absorption capacity, it can be said that the amount of sand behind the plate influences the energy absorption behaviour of the plate when subjected to compressive loads from the compressed sand in front.

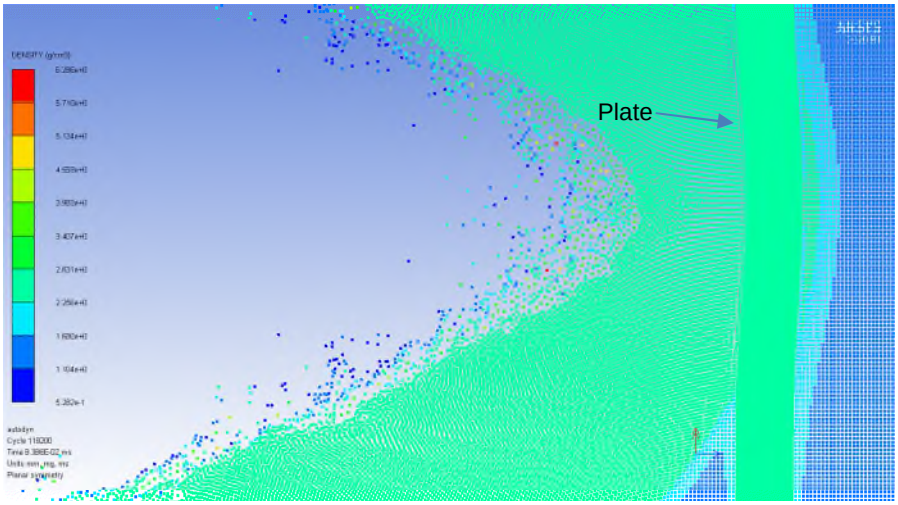

Figure 14 Rear localised sand compression induced through plate deformation due to localised loading by compressed sand following impact by 12mm steel projectile at 850m/s.

2.4 Effect of Plate Thickness

The plate thickness directly influences the mass of the protection system and the areal density of the system. Additionally, the thickness of the plate also influences the energy absorption behaviour of both, the sand and plate. Based on the material being used, the thickness of the plate increases the penetration resistance provided by the system. An increase in penetration resistance means that the energy from the projectile is absorbed and dissipated in less time. Consequently, this has the potential to make the protection system capable of surviving multiple hits. Performance of the protection system was observed for plate thickness of 15mm and 25mm. It must also be noted that conventionally, plates of 15 or 25mm are not used for materials like plexiglass or polycarbonate. They have been considered in this simulation study for the purpose of uniformity.

Figures 12 and 13 show the change in specific internal energy of plates of different materials and thicknesses. While the profile for energy absorption is largely similar for both plate thicknesses, it is important to highlight that the magnitude is not. Since the highest energy absorption was observed for plates placed at 226mm, the comparison of plates of different thicknesses has been focused on those simulations. From Figures 12 and 13, 25mm plates had a higher

rise in specific internal energy when subjected to compressive loading from the sand. This shows that 25mm plates absorb 0.1-27% more energy than 15mm plates at the time of initial contact (0.07-0.075ms) depending on the material of the plate. Furthermore, a positive correlation can be drawn between the plate thickness and increased areal density of the system. In addition to that, increasing the thickness of the plate increases the mass of the obstruction faced by the moving sand. The increased mass of the plate allows for a higher specific internal energy after the initial interaction between the plate and sand. Between 0.075ms and 0.1ms, the 25mm plates retained up to 18% more energy as compared to the 15mm plates. This adds value to the correlation between plate thickness and the energy absorption characteristics of the system.

Figures 10 and 11 show the change in specific internal energy of sand when it impacts plates of different thicknesses. As mentioned earlier, the profile of specific internal energy change in both cases was largely similar with the primary difference in their respective magnitudes. In both cases, sand had the greatest energy absorption when a steel plate was used. This is because the steel plate has the lowest energy absorption as compared to plates of other materials. The steel plate deforms the least and as a result, does the least work when under compressive loading. Consequently, the sand undergoes more densification resulting in the increase in its specific internal energy. Subsequently, this trend is observed with cases where aluminium and concrete plates are used as well. Since materials of these plates do not deform as much as plexiglass or polycarbonate, the sand absorbs and dissipates a large part of the energy supplied by the projectile. With regards to the thickness of the plate, the 25mm plate deforms less than the 15mm plate when subject to compressive loading. This lack of deformation causes a larger compression of sand resulting in the higher energy absorption. The benefit of the reduced deformation is that it adds to the system’s ability to resist attack and can potentially improve the system’s multi-hit capability.

2.5 Effect of Areal Density

The areal density defines the mass of the protection system with respect to its size. With regards to this study, adding a plate into the sandbag changes its areal density because part of the sand is replaced by a solid plate. The area of the protection system has been kept constant (300mm x 300mm) to maintain focus on the modifications to the sandbag. This factor is considered because the mass plays a role in the energy absorption characteristics of the system and in turn the penetration resistance provided by the system. Additionally, it must be acknowledged that the mass of the protection system (sand and plate combined) must be controlled to make it more viable to transport and deploy. Table 3 shows the mass of the sandbag when plates of different materials and different thickness are added to it.

Table 3 Mass of the protection system with plates of different thickness and material

15mm Plate						
	Conventional sandbag	Aluminium	Concrete	Plexiglass	Polycarbonate	Steel
Plate mass (kg)	0	0.012	0.010	0.005	0.005	0.035
Sand mass (kg)	0.151	0.143	0.143	0.143	0.143	0.143
Total mass (kg)	0.151	0.155	0.153	0.148	0.148	0.178
25mm Plate						
	Conventional sandbag	Aluminium	Concrete	Plexiglass	Polycarbonate	Steel
Plate mass (kg)	0	0.020	0.017	0.008	0.009	0.059

Sand mass (kg)	0.151	0.138	0.138	0.138	0.138	0.138
Total mass (kg)	0.151	0.158	0.155	0.147	0.147	0.197

Table 4 Areal Density of the protection system with plates of different thickness and material

Areal Density (kg/m^2)/Material	Conventional sandbag	Aluminium	Concrete	Plexiglass	Polycarbonate	Steel
15mm plate	1.674	1.725	1.706	1.650	1.650	1.982
25mm plate	1.674	1.760	1.727	1.633	1.635	2.187

The density of the plate material plays an important role in the determination of areal density of the system. An increase in areal density was observed when materials denser than sand were added to the system. Replacing sand with another material in a constant area (15mmx300mm and 25mmx300mm) changes the overall mass of the system. Therefore, if the sand is replaced by a denser material, the mass of the system increases and consequently the areal density as well. Polycarbonate and plexiglass were the two materials whose densities were less than that of sand. As a result, adding plates of these materials resulted in reduction of areal density by 1.5-2.5% as compared to the conventional system. Subsequently, the addition of 15mm and 25mm steel plates had the maximum increase in areal density of the system by 18.4% and 30.6% respectively. Polycarbonate and plexiglass plates absorb the most energy during impact, and the use of these plates reduces the areal density of the sandbag. But these plates deform very easily and cannot be used as standalone modifications. It is of value to recognise that the use of these materials in sandwich structures and composites has the potential to provide a comparable level of protection without the extensive deformation of the plate [33,46,49].

Furthermore, correlations can be made between the energy absorption of sand and the areal density of the system. At the time of impact (0.07ms-0.1ms), sand had the highest specific internal energy when a steel plate was added to the system. The contributing factors to this behaviour are the rigid steel plate and the increased mass of the overall system aiding the penetration resistance provided by the system by increasing the compaction of sand as compared to other systems. Systems with aluminium and concrete plates had the second and third highest areal densities, respectively. Consequently, the second and third highest specific internal energy in sand was observed in systems with aluminium and concrete plates, respectively. Additionally, it is important to highlight that systems with polycarbonate and plexiglass plates showed a lower specific internal energy of sand as compared to conventional systems. The reason behind this is the rapid dissipation of energy to the plate resulting in its deformation.

With respect to the plates, it was observed that systems with higher areal density showed lesser deformation of plates as well as lower change in specific internal energy. While a heavier system tends to absorb energy better, the contribution of the plate in this process is that of enabling densification of sand, rather than aiding the process of energy absorption. Based on this premise, it was observed that polycarbonate and plexiglass plates had the highest energy absorption on impact and the largest deformations. Subsequently, systems with the concrete plates showed a relatively high specific internal energy change with lesser deformation than the plastic plates.

In addition to the energy absorption behaviour of these systems, it is essential to keep in mind their practical viability. While a modified sandbag can absorb energy better than the conventional kind, factors such as the weight of the system and the logistical requirement for its setup must be considered. Conventionally, plexiglass and polycarbonate plates are not 15mm or 25mm thick (typical thickness of about 4-6mm [46]), which means that if these plates are to be used, it has the potential to drive up the manufacturing cost of the protection system. Subsequently concrete, aluminium and steel plates are relatively easy to manufacture, but create a logistical burden in terms of transport and setup time

due to their heavy weight. While a HESCO bag is already heavy, the addition of a plate further increases that weight. The increase in weight is not significant given the scale of deployment of this system but there is a significant change in the energy absorption characteristics. The selection criteria for a protection system of this kind should factor in a balance between its weight, areal density, and the rise in cost of the system (if any).

2.6 Experimental Validation of Simulations

Lab scale experiments were conducted to validate the simulations. 15mm Aluminium plates were used in the experiment because simulations with aluminium showed high energy absorption and penetration resistance. Plate location of 226mm was selected because all the simulations showed higher energy absorption performance compared to cases with plates at 236mm and 256mm. While sandbags with concrete and aluminium plates showed comparable penetration resistance, sandbags with aluminium had a higher areal density, thus making them the preferred choice for experiments. Table 5 shows the results from the lab scale firings for sand targets with and without a plate.

Table 5 Observations from gas gun firings of steel projectile into a sandbag and modified sandbag

Setup	He Gas Pressure (bar)	Impact Velocity (m/s)	Penetration Depth (mm)
Sand only	56	867	168
Sand only	56	867	265
15mm Al plate	56	867	196
15mm Al plate	56	867	205

From table 5, the projectile does not interact with the plate placed at 226mm. The distance between the plate and projectile is between 21-30mm. It was also observed that there was a large variation in results when the projectile was fired at the target without the presence of a plate. In some cases, the projectile changed direction during impact and was vertically shot out of the sand resulting in an inaccurate measure of penetration depth. In the successful control firings, the projectile penetrated up to 265mm of sand. This observation suggests that the presence of a plate in sand reduces projectile penetration up to approximately 26%. The results of these experiments can validate the simulation results because similar observations were made in both cases. In both cases, the projectile does not penetrate the sand enough to directly interact with the plate, thus suggesting an increased penetration resistance when a plate is present in the sand. This claim is further reinforced by the observations made in the computer simulations which suggest that the compaction of sand coupled with the improved energy dissipation provided by the plate increase the overall penetration resistance of the protection system.

3 Conclusion

The change in protection performance of a conventional sandbag after it has been modified by adding a plate has been simulated. Different plate materials, locations and plate thicknesses were compared and the change in energy absorption characteristics of the system were studied and analysed. The following conclusions can be drawn from this simulation study:

- Adding a plate to the sandbag reduced the penetration depth by 15mm given the 0.1ms timescale. The same reduction in penetration was observed for all modified systems.
- Simulation studies showed that the energy absorption of sand increased when a plate was added in the compressed sand in front of the projectile. The plate absorbs the energy from the compressed sand resulting in its deformation. This deformation causes the compression of a larger area of sand behind the plate.
- It was noted that a 25mm plate when placed at 226mm from point of impact enables better compaction of the sand, thus enabling better energy absorption characteristics of the system.
- Polymer materials such as polycarbonate and plexiglass tend to absorb the most energy when subject to loading but deform very easily too. Consequently, Steel and aluminium are rigid materials that do not deform easily but do not adequately aid energy absorption in the protection system. Subsequently, it was noted that concrete and aluminium had comparable areal density and energy absorption characteristics to polycarbonate but did not deform as much under compressive loading, thus making them an ideal choice for plate material in modified sandbags.
- Experiments were conducted using a modified sand target with a 15mm Aluminium plate to validate the simulations. Similar penetration behaviour was observed in the simulation and the experiments, thus validating the simulation results.

ACKNOWLEDGEMENTS

The authors would like to thank Mr. Andrew Roberts, Mr. Alan Peare and Mr. Eric Chin for providing the IT support and resources in the duration of this project.

REFERENCES

[1] A. Richardson, M. Heather, Improving the performance of concrete using 3D fibres, Procedia Eng. 51 (2013) 101–109. https://doi.org/10.1016/j.proeng.2013.01.016.

[2] W.G. Proud, D.J. Chapman, D.E. Eakins, The stress and ballistic properties of granular materials, AIP Conf. Proc. 1793 (2017). https://doi.org/10.1063/1.4971705.

[3] National University of Singapore, Sand absorbs high-speed ballistic impact better than steel, Phys.Org. (2016) 1–3.

[4] A. Haris, V.B.C. Tan, Experimental study on compaction effects on the ballistic resistance of sandbags, Int. J. Impact Eng. 142 (2020) 103609. https://doi.org/10.1016/j.ijimpeng.2020.103609.

[5] P. Cormie, David Mays, Geoff Smith, Blast Effects on Buildings - (2nd Edition) - Knovel, 2nd ed., ICE Publishing, 2009. https://app.knovel.com/web/toc.v/cid:kpBEBE0001/viewerType:toc//root_slug:blast-effects-buildings/url_slug:blast-effe-loading?=undefined&issue_id=kpBEBE0001&hierarchy= (accessed December 13, 2019).

[6] W.D. Reinhart, T.F. Thornhill III, L.C. Chhabilidas, T.J. Vogler, J.L. Brown, Shock response of dry sand, 2007.

[7] J.I. Perry, C.H. Braithwaite, N.E. Taylor, A.P. Jardine, The significance of grain morphology and moisture content on the response of silica sand to ballistic penetration, Appl. Phys. Lett. 115 (2019). https://doi.org/10.1063/1.5114881.

[8] P. Vivek, T.G. Sitharam, Laboratory scale investigation of stress wave propagation and vibrational characteristics in sand when subjected to air-blast loading, Int. J. Impact Eng. 114 (2018) 169–181. https://doi.org/10.1016/j.ijimpeng.2018.01.003.

[9] J.L. Brown, T.J. Vogler, D.E. Grady, W.D. Reinhart, L.C. Chhabildas, T.F. Thornhill, Dynamic compaction of sand, AIP Conf. Proc. 955 (2007) 1363–1366. https://doi.org/10.1063/1.2832977.

[10] HESCO, HESCO MIL Barriers, (2020). https://www.hesco.com/products/mil-units/mil/ (accessed September 4, 2020).

[11] T. Elshenawy, M.A. Seoud, G.M. Abdo, Ballistic Protection of Military Shelters from Mortar Fragmentation and Blast Effects using a Multi-layer Structure, Def. Sci. J. 69 (2019) 538–544. https://doi.org/10.14429/dsj.69.13269.

[12] K. Ahmed, A.Q. Malik, I.R. Ahmad, Heterogeneous lightweight configuration for protection against 7.62 × 39 mm bullet impact, Int. J. Prot. Struct. 10 (2019) 289–305. https://doi.org/10.1177/2041419619839216.

[13] S.C. Chian, B.C.V. Tan, A. Sarma, Projectile penetration into sand: Relative density of sand and projectile nose shape and mass, Int. J. Impact Eng. 103 (2017) 29–37. https://doi.org/10.1016/j.ijimpeng.2017.01.002.

[14] T. Børvik, A. Burbach, H. Langberg, M. Langseth, On the ballistic and blast load response of a 20ft ISO container protected with aluminium panels filled with a local mass - Phase II: Validation of protective system, Eng. Struct. 30 (2008) 1621–1631. https://doi.org/10.1016/j.engstruct.2007.10.011.

[15] M. Omidvar, M. Iskander, S. Bless, Soil-projectile interactions during low velocity penetration, Int. J. Impact Eng. 93 (2016) 211–221. https://doi.org/10.1016/j.ijimpeng.2016.02.015.

[16] A. Cave, S. Roslyakov, M. Iskander, S. Bless, Design and Performance of a Laboratory Pneumatic Gun for Soil Ballistic Applications, Exp. Tech. 40 (2016) 541–553. https://doi.org/10.1007/s40799-016-0055-3.

[17] S.J. Bless, D.T. Berry, B. Pedersen, W. Lawhorn, Sand penetration by high-speed projectiles, AIP Conf. Proc. 1195 (2009) 1361–1364. https://doi.org/10.1063/1.3295061.

[18] J.P. Borg, P. Sable, H. Sandusky, J. Felts, In situ characterization of projectile penetration into sand targets, AIP Conf. Proc. 1793 (2017). https://doi.org/10.1063/1.4971696.

[19] M. Esmaeili, B. Tavakoli, Finite element method simulation of explosive compaction in saturated loose sandy soils, Soil Dyn. Earthq. Eng. 116 (2019) 446–459. https://doi.org/10.1016/j.soildyn.2018.09.048.

[20] J.R. Finn, M. Li, S. V. Apte, Particle based modelling and simulation of natural sand dynamics in the wave bottom boundary layer, J. Fluid Mech. 796 (2016) 340–385. https://doi.org/10.1017/jfm.2016.246.

[21] Y. Li, D.M. Kelly, M. Li, J.M. Harris, J.R. Finn, An Euler-Lagrange approach to model local scour and sand transport, 2015.

[22] W. Zhang, X. Huang, Y. Qi, D. Li, J. Tao, W. Huang, Experimental investigation on ballistic stability of high-speed projectile in sand, AIP Conf. Proc. 1793 (2017). https://doi.org/10.1063/1.4971587.

[23] D. Nandlall, G. Wong, A Numerical Analysis of the Effect of Erosion Strain on Ballistic Performance Prediction, (1999) 28.

[24] J. Spencer, The Most Effective Weapon on the Modern Battlefield is Concrete | RealClearDefense, Mod. War Inst. (2016). https://www.realcleardefense.com/articles/2016/11/15/the_most_effective_weapon_on_the_modern_battlefield_is_concrete_110348.html (accessed May 21, 2020).

[25] L. Laine, A. Sandvik, Derivation of Mechanical properties for Sand, in: 4th Asia-Pacific Conf. Shock Impact Loads Struct. CI-Premier PTE LTD, Singapore, 2001: pp. 361–368.

[26] Johnson, Cook, Selected hugoniots: EOS, in: 7th Int. Symp. Ballist., 1969.

[27] D. Steinberg, Equation of state and strength properties of selected materials, Lawrence Livermore National Laboratory, 1996.

[28] W. Riedel, N. Kawai, K. ichi Kondo, Numerical assessment for impact

strength measurements in concrete materials, Int. J. Impact Eng. 36 (2007) 283–293. https://doi.org/10.1016/j.ijimpeng.2007.12.012.

[29] W. Riedel, K. Thoma, S. Hiermaier, Penetration of Reinforced Concrete by BETA-B-500 Numerical Analysis Using a New Macroscopic Concrete Model for Hydrocodes, in: Proc 9, 1999: p. 8.

[30] M.G. Vigil, Projectile Impact Hugoniot Parameters for Selected Materials, 1989. https://doi.org/10.2172/5658829.

[31] S.M. Walley, J.E. Field, Strain rate sensitivity of polymers in compression from low to high rates, DYMAT J. 1 (1997) 16.

[32] G.R. Johnson, W.H. Cook, Fracture characteristics of three metals subjected to various strains, strain rates, temperatures and pressures, Eng. Fract. Mech. 21 (1985) 31–48. https://doi.org/10.1016/0013-7944(85)90052-9.

[33] Sangamesh, K.S. Ravishankar, S.M. Kulkarni, Ballistic Impact Study on Jute-Epoxy and Natural Rubber Sandwich Composites, Mater. Today Proc. 5 (2018) 6916–6923. https://doi.org/10.1016/j.matpr.2017.11.353.

[34] E.A. Chernyshov, A.D. Romanov, E.A. Romanova, V. V. Myl'nikov, Development of Ballistic Protection Based on Precipitation-Hardened Composite Material, Met. Sci. Heat Treat. 59 (2018) 741–744. https://doi.org/10.1007/s11041-018-0220-7.

[35] G.S. Collins, An introduction to hydrocode modeling, Appl. Model. Comput. Group, Imp. Coll. London. (2002).

[36] D.J. Benson, Computational methods in Lagrangian and Eulerian hydrocodes, Comput. Methods Appl. Mech. Eng. 99 (1992) 235–394. https://doi.org/10.1016/0045-7825(92)90042-I.

[37] P. Cossins, The Gravitational Instability and its Role in the Evolution of Protostellar and Protoplanetary Discs, University of Leicester, 2010. https://doi.org/10.1111/j.1365-2966.2010.17158.x.

[38] J.A. Zukas, Introduction to hydrocodes, 1st ed., Elsevier, Amsterdam; Boston, 2004.

[39] M.Y.. Bangash, Impact and Explosion, 1st ed., Blackwell Scientific Publications, Oxford, 1993.

[40] P. Smith, J. Hetherington, Blast and Ballistic Loading of Structures, 1st ed., Butterworth Heinemann, Oxford, 1994.

[41] Polycarbonate (PC) Plastic: Properties, Uses, & Structure - Guide, Omnexus. (2018). https://omnexus.specialchem.com/selection-guide/polycarbonate-pc-plastic (accessed August 5, 2020).

[42] H. Zhu, K.C. Jha, R.S. Bhatta, M. Tsige, A. Dhinojwala, Molecular structure of poly(methyl methacrylate) surface. I. combination of interface-sensitive infrared-visible sum frequency generation, molecular dynamics simulations, and ab initio calculations, Langmuir. 30 (2014) 11609–11618. https://doi.org/10.1021/la502333u.

[43] M. Belali-Owsia, M. Bakhshi-Jooybari, S.J. Hosseinipour, A.H. Gorji, A new process of forming metallic bipolar plates for PEM fuel cell with pin-type pattern, Int. J. Adv. Manuf. Technol. 77 (2015) 1281–1293. https://doi.org/10.1007/s00170-014-6563-3.

[44] Y. Rui, A. Subic, M. Takla, C. Wang, A. Niehoff, N. Hamann, G.P. Brueggemann, Biomimetic design of lightweight vehicle structures based on animal bone properties, Adv. Mater. Res. 633 (2013) 3–14. https://doi.org/10.4028/www.scientific.net/AMR.633.3.

[45] J. Feng, W. Sun, L. Wang, L. Chen, S. Xue, W. Li, Terminal ballistic and static impactive loading on thick concrete target, Constr. Build. Mater. 251 (2020) 118899. https://doi.org/10.1016/j.conbuildmat.2020.118899.

[46] I.G. Crouch, The Science of Armour Materials, 1st ed., Woodhead Publishing, 2017.

[47] P.J. Hazell, ARMOUR: Materials, theory, and design, CRC Press, 2015.

https://doi.org/10.1201/b18683.

[48] D. Brehm, Cement’s basic molecular structure finally decoded | MIT News, MIT News. (2009). http://news.mit.edu/2009/cement-0909 (accessed August 4, 2020).

[49] M.S. Aly-Hassan, A new perspective in multifunctional composite materials, Elsevier Inc., 2015. https://doi.org/10.1016/B978-0-323-26434-1.00002-7.

APPENDICES

Appendix A Gurney Calculations for Projectile Velocity Determination

155mm Shell:

- Total weight: 43.2kg
- Comp B weight (C): 6.6kg
- Case Weight (M): 36.6kg
- $\sqrt{2E}$ of Comp B: 2700m/s

Fragment data:

- Diameter: 12mm
- Density of Steel 1006: 7896kg/m^3
- Volume: 9.048 x 10^{-7} m^3
- Mass: 7.24 x 10^{-3} kg
- C_d (rough sphere): 0.48
- V_s: 850m/s

$$V_o = \sqrt{2E}\,(\frac{M}{C}+\frac{1}{2})^{-0.5}$$

$$V_o = 2700\,(\frac{36.6}{6.6}+\frac{1}{2})^{-0.5} = 1050.97\,m/s = V_d$$

$$V_s = V_d e^{-C_d \rho_{air} S(\frac{A}{2m})}$$

$$850 = 1050.97 e^{-0.48\times 1.225\times S(\frac{4.52\times 10^{-4}}{2(7.24\times 10^{-3})})}$$

$$\frac{850}{1050.97} = e^{-0.018S}$$

$$-0.212 = -0.018S$$

$$\boldsymbol{S \approx 11.7m}$$

Numerical modelling study of a modified sandbag system for ballistic protection

Thawani, Bonny

2021-06-05

Thawani B, Hazael R, Critchley R. (2021) Numerical modelling study of a modified sandbag system for ballistic protection. Journal of Computational Science, Volume 53, July 2021, Article number 101403

https://doi.org/10.1016/j.jocs.2021.101403